Plasma Polymerization of Tetramethylsilane

J. L. C. Fonseca, D. C. Apperley,† and J. P. S. Badyal*

Department of Chemistry, Science Laboratories, Durham University, Durham DH1 3LE, England

Received July 14, 1993®

Plasma polymerization of tetramethylsilane ($Si[CH_3]_4$) over short periods results in the formation of a continuous organosilicon layer, whereas longer deposition times produce a fine brown powder. As-deposited and aged plasma polymer coatings/powders have been characterized by XPS, FTIR, XRD, and solid-state NMR. The carbosilane plasma polymer is found to mainly consist of a random network of $-[CH_3]_nSiH_m-$ linkages.

Introduction

Injection of molecular gases into a low-temperature glow discharge can generate solid-forming species.[1] Typically such nonequilibrium plasmas consist of energetically hot electrons, cold ions, radicals, neutrals, and photons. This combination of reactive species may give rise to either substrate etching or thin-film deposition depending upon the gas and excitation energy employed. Glow discharge polymerization reactions have been investigated for over 20 years; however, the fundamental understanding of such processes remains poor in comparison to conventional polymerization.[1,2]

Plasma-polymerized organosilicon layers are of potential interest for a variety of applications. These include biocompatible coatings,[3] integrated optical circuitry,[4,5] semiconductor device fabrication,[6] as precursors for the synthesis of silicon carbide,[7] moisture barrier coatings,[8] corrosion resistant films,[9] photoresists,[10] and as adhesion promoters between glass fibers and polymer matrices.[11,12] Tetramethylsilane ($Si[CH_3]_4$),[13,14] phenylsilane ($[C_6H_5]SiH_3$),[15] and trimethylvinylsilane ($[CH_3]_3Si[CHCH_2]$)[16] are among some of the carbosilane monomers previously studied. Silylmethyl groups $[CH_3]_xSi$ (x = 1, 2, 3), and weak Si–Si linkages in saturated organosilicon precursors are understood to play a key role during plasma polymerization.[17] For instance, it has been shown that hexamethyldisilane ($[CH_3]_3Si-Si[CH_3]_3$) is much more susceptible toward glow discharge deposition than its monosilicon counterparts.[18]

In this article, the plasma polymerization of tetramethylsilane (TMS) over a range of energies is described. Both thin layers and powders have been synthesized. Freshly deposited and aged materials have been characterized by XPS, FTIR, NMR, and XRD, in conjunction with UV emission analysis of the TMS glow discharge itself. This combination of analyses on the same product offers a much deeper insight into the polymerization and structural aspects of these carbosilicon materials.

Experimental Section

Tetramethylsilane (TMS, 99.9% Aldrich Chemical Co.) was degassed by multiple freeze–pump–thaw cycles. Two types of substrate were used: low-density polyethylene film for thin plasma polymer coatings (LDPE, Metal Box, 0.1–mm thickness), and glass slides for bulk powder product (1-mm thickness). Both were cleaned with isopropyl alcohol and dried prior to use.

Glow discharge experiments were carried out in an electrodeless cylindrical glass reactor (4.5-cm diameter, 490 cm^3 volume) enclosed in a Faraday cage. It was fitted with a monomer inlet, a Pirani pressure gauge, and a 47 L min^{-1} two-stage rotary pump attached to a liquid nitrogen cold trap. A 13.56-MHz radio frequency (rf) source was inductively coupled to a copper coil (4-mm tube diameter, nine turns, spanning 11.0–18.5 cm from the monomer inlet) via a matching network. Monomer flow rate was controlled using a fine needle valve. Glow discharges at less than 5 W of power were sustained by pulsing the plasma.[19] All joints were grease-free. Experiments which investigated the effects of W/F_M, and time upon deposition used a fixed substrate position of 6.5 cm from the monomer inlet. In the case of bulk material studies, glow discharge parameters corresponding to maximum deposition rate were used (W/F_M = 280 MJ/kg, as determined from ATR-FTIR). Monomer and leak mass flow rates were measured assuming ideal gas behavior.[20]

A typical experimental run consisted of first scrubbing the reactor with detergent, rinsing with isopropyl alcohol, and drying, followed by a high-power (50 W) air plasma treatment for 60 min. This latter step was done in the presence of glass substrates, but in the absence of polyethylene film, since oxygen glow discharges are renowned for their ability to oxidize polymer

† Industrial Research Laboratories, University of Durham, DH1 3LE, England.

* To whom correspondence should be addressed.

® Abstract published in *Advance ACS Abstracts,* October 15, 1993.

(1) Yasuda, H. *Plasma Polymerization*; Academic Press: Orlando, FL, 1985.
(2) Beidrman, H.; Osada, Y. *Adv. Polym. Sci.* **1990**, *95*, 57.
(3) Sharma, A. K.; Yasuda, H. *Thin Solid Films* **1983**, *171*, 245.
(4) Tien, P. K.; Smolinsky, G.; Martin, R. *J. Appl. Opt.* **1972**, *11*, 637.
(5) Tyczkowski, J.; Odrobina, E.; Kazimierski, P.; Bassler, H.; Kisiel, A.; Zema, N. *Thin Solid Films* **1992**, *209*, 250.
(6) Larkin, D. J.; Interrante, L. V. *Chem. Mater.* **1992**, *4*, 22.
(7) Konotek, O.; Loffler, F. *Mater. Sci. Eng.* **1991**, *A140*, 655.
(8) Sacher, E.; Klemberg-Sapieha, J. E.; Schreiber, H. P.; Wertheimer, M. R. *J. Appl. Polym. Sci., Appl. Polym. Symp.* **1984**, *38*, 149.
(9) Cho, D. L.; Yasuda, H. *J. Appl. Polym. Sci., Appl. Polym. Symp.* **1988**, *42*, 233.
(10) Horn, M. W.; Pang, S. W.; Rothschild, M. *J. Vac. Sci. Technol. B* **1990**, *8*, 1493.
(11) Lin, T. J.; Chun, B. H.; Yasuda, H. K.; Yang, D. J.; Antonelli, J. A. *J. Adhesion Sci. Technol.* **1991**, *5*, 893.
(12) Krishnamurthy, V.; Kamel, I. L.; Wei, Y. *J. Appl. Polym. Sci.* **1989**, *38*, 605.
(13) Nguyen, V. S.; Underhill, J.; Fridmann, S.; Pan, P. *J. Electrochem. Soc.* **1985**, *132*, 1925.
(14) Park, S. Y.; Kim, N.; Hong, S. I.; Sasabe, H. *Polym. J.* **1990**, *22*, 242.
(15) Laoharojanaphand, P.; Lin, T. J.; Stoffer, J. O. *J. Appl. Polym. Sci.* **1990**, *40*, 369.
(16) Kruse, A.; Hennecke, M.; Baalmann, A.; Schlett, V.; Stuke, H. *Ber. Bunsen-Ges. Phys. Chem.* **1991**, *11*, 1376.
(17) Inagaki, N.; Kishi, A. *J. Polym. Sci., Polym. Chem. Ed.* **1983**, *21*, 2335.
(18) Fonseca, J. L. C.; Badyal, J. P. S. *Macromolecules* **1992**, *25*, 4730.
(19) Clark, D. T.; Shuttleworth, D. *J. Polym. Sci., Polym. Chem. Ed.*, **1980**, *18*, 27.
(20) Ehrlich, C. D.; Basford, J. A. *J. Vac. Sci. Technol. A* **1992**, *10*, 1.

0897-4756/93/2805-1676$04.00/0 Published 1993 by the American Chemical Society

surfaces.[21] Then the reactor was pumped down to a base pressure of 2×10^{-2} Torr, and a leak rate lower than 2.6×10^{-10} kg/s. Subsequently the TMS monomer was introduced into the reaction chamber at 1×10^{-1} Torr pressure and a mass flow rate (F_M) of 3.6×10^{-8} kg/s (i.e., at least 99.3% of total mass flow is the organosilane precursor). After allowing 5 min for purging, the glow discharge was ignited. Upon termination of deposition, the reactor was evacuated back down to its original base pressure for at least 5 min. Finally the system was let up to atmosphere, and the appropriate analytical measurement undertaken. Characterization was carried out on freshly deposited plasma polymer and on material that had been left to age for 1 month in air.

X-ray photoelectron spectra were acquired on a Kratos ES200 surface analysis instrument operating in the fixed retarding ratio (22:1) analyzer mode. Magnesium Kα X-rays were used as the photoexcitation source with an electron take-off angle of 30° from the surface normal. Instrument performance was calibrated with respect to the gold $4f_{7/2}$ level at 83.8 eV with a full width at half-maximum (fwhm) of 1.2 eV. No radiation damage was observed during the typical time scale involved in these experiments. An IBM PC computer was used for data accumulation and component peak analysis (assuming linear background subtraction and Gaussian fits with fixed fwhm). All binding energies are referenced to the hydrocarbon component at 285.0 eV.[22] Instrumentally determined sensitivity factors for unit stoichiometry were taken as C(1s):O(1s):Si(2p) equals 1.00:0.55:1.05.

Infrared absorbance spectra of TMS monomer, powdered material, and coated polyethylene film were taken on a FTIR Mattson Polaris instrument. Plasma polymer powder was mixed with dried KBr, then pressed into a disk, and characterized by the transmission method. These results were compared with TMS diluted in CCl_4 (3% weight/volume solution). Samples prepared with polyethylene substrate were mounted onto a variable angle attenuated total reflection (ATR) cell fitted with a KRS-5 crystal. An incident beam angle of 45° was used, which resulted in 14 internal reflections.[23] Typically, 100 scans were acquired at a resolution of 4 cm^{-1}.

Solid-state NMR spectra were taken on a Varian VXR-300 spectrometer equipped with a Doty Scientific magic-angle-spinning (MAS) probe. ^{29}Si NMR signals were recorded at 59.6 MHz, and ^{13}C at 75.4 MHz. In both cases, tetramethylsilane was used as the chemical shift reference.

A computer controlled UV emission spectrometer based upon a Czerny-Turner type monochromator was used for plasma glow analysis. This instrument could scan the spectrum continuously from 180 to 500 nm at 0.5-nm resolution.

Elemental microanalysis was done on a Carlo Erba elemental analyzer (Model 1106). A Philips X-ray diffractometer (Model PW1009/80) fitted with a Cu Kα ($\lambda = 1.5443$ Å) tube and a Debye-Scherrer camera were used to evaluate whether the collected plasma powder possessed any crystalline character.

Results

Short deposition times resulted in a uniform coating, whereas longer periods (6 h) produced a substantial amount of noncrystalline powder. The deposit was brown, and did not visibly change in appearance with time. Elemental microanalysis of plasma polymer powder produced at the maximum deposition rate (W/F_W = 280 MJ/kg) yielded a H/C ratio of 1.9.

X-ray Photoelectron Spectroscopy. The C(1s) XPS envelope of a thick layer of TMS plasma polymer coated onto a glass substrate (Figure 1) contains a maximum at 285.0 eV related to the presence of C–C, C–H, and C–Si environments.[24,25] The Si(2p) region shows a single feature

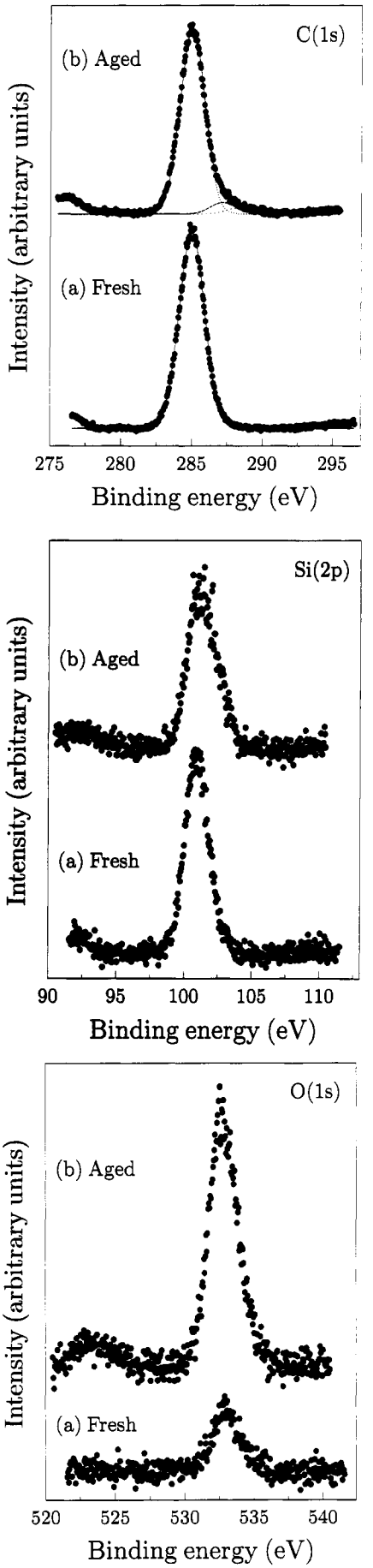

Figure 1. C(1s), Si(2p), and O(1s) XPS spectra of a thick layer of TMS plasma polymer (W/F_M = 280 MJ/kg, 10 min, and 6.5 cm from monomer inlet): (a) fresh and (b) aged in air for 1 month.

(21) Shard, A. G.; Badyal, J. P. S. *Macromolecules* **1992**, *25*, 2053.
(22) Johansson, G.; Hedman, J.; Berndtsson, A.; Klasson, M.; Nilsson, R. *J. Electron Spectrosc.* **1973**, *2*, 295.
(23) Graf, R. T.; Koekig, J. L.; Ishida, H. *Introduction to Optics and Infrared Spectroscopic Techniques*, in *Fourier Transform Infrared Characterization of Polymers*; Ishida, H., Ed.; Plenum Press: New York, 1987.

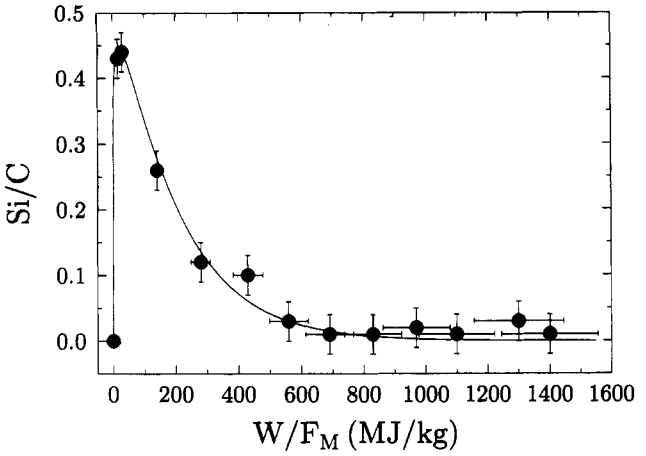

Figure 2. Dependence of Si/C ratio upon W/F_M for freshly deposited TMS plasma polymer (10 min, and 6.5 cm from monomer inlet).

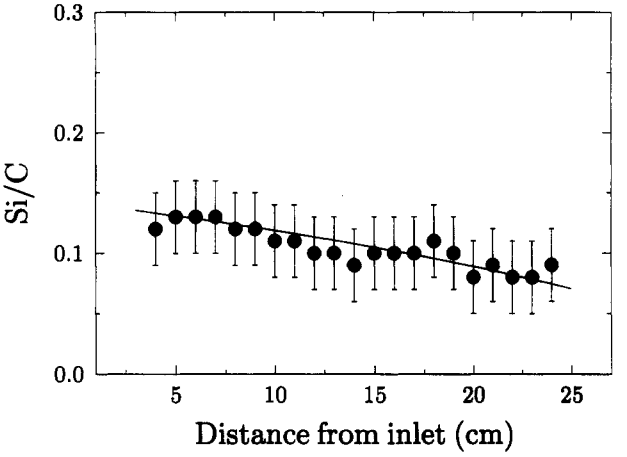

Figure 3. Variation in Si/C ratio as function of distance from monomer inlet (W/F_M = 280 MJ/kg and 10 min).

centered at 100.7 eV, which indicates the presence of Si–H and Si–C environments.[24-26] A small peak at a 533.0 eV related to O(1s) level was observed in the spectra of fresh plasma polymer films. The oxygen content, calculated as a fraction of total carbon, silicon and oxygen amount, was less than 3 at. %. This probably originates from trapped free radicals in the plasma polymer reacting on air exposure during transport from the deposition chamber to the X-ray photoelectron spectrometer. XPS analysis during argon ion sputter depth profiling confirmed that this small amount of oxidation was just localized at the product surface. Corresponding C(1s), Si(2p), and O(1s) spectra taken following prolonged exposure to air (1 month) displayed a significant degree of oxidation. Oxygen content was much greater in this case (11%). A pronounced shoulder is evident in the C(1s) envelope which can be attributed to the occurrence of C–O (286.6 eV) and >C=O (287.9 eV) functionalities.[27] A corresponding shift in the Si(2p) peak toward higher binding energy (101.2 eV) is seen, this is probably due to the presence of Si–O (102.2 eV) and O–Si–O (104.0 eV) silicon environments.[28]

Figure 2 summarizes the influence of W/F_M upon Si/C ratio for freshly deposited TMS plasma polymer layers onto a polyethylene substrate. The oxygen content measured in these experiments was consistent with values reported above for glass substrates (i.e., less than 3%), and therefore heating of the polyethylene substrate by the RF field can be ruled out. No silicon species were detected in the absense of a glow discharge. The Si/C atomic ratio passes through a maximum with increasing W/F_M and then drops to zero. Related measurements show that the Si/C ratio decreases on moving downstream from the monomer inlet (Figure 3). Furthermore, the Si/C ratio is found to be independent of deposition time, and therefore the coating must be homogeneous.

Activation of polyethylene film with an argon plasma (5–50 W), followed by exposure to TMS monomer (in the absence of a glow discharge) did not result in any silicon uptake by the substrate. Therefore organosilicon deposition must be terminated at the precise moment at which the plasma is extinguished.

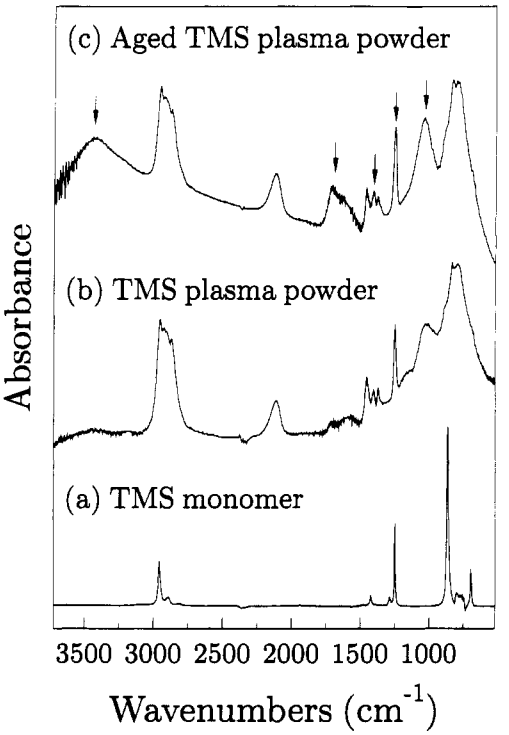

Figure 4. FTIR transmission spectra of (a) TMS monomer, (b) fresh TMS plasma powder (W/F_M = 280 MJ/kg), and (c) aged TMS plasma powder (W/F_M = 280 MJ/kg). Changes in absorbances during ageing of plasma polymer are indicated by arrows.

Table I. Infrared Absorption Bands for Tetramethylsilane[29]

absorbance/cm^{-1}	assignment
2955	C–H asymmetrical stretching in CH_3
2891	C–H symmetrical stretching in CH_3
1248	CH_3 symmetric bending in $Si[CH_3]_n$
864	CH_3 rocking in $Si[CH_3]_n$
694	Si–C stretching

FTIR Spectroscopy. Figure 4 is a compilation of the FTIR transmission spectra of TMS monomer and fresh and aged TMS plasma polymer powder. Characteristic absorption bands for TMS are assigned in Table I.

The strong absorbances for freshly deposited TMS plasma polymer powder are listed in Table II. Exposure

(24) Inagaki, N.; Katsuoka, H. *J. Membr. Sci.* **1987**, *34*, 297.
(25) Clark, D. T.; Feast, W. J. *J. Macromol. Sci., Rev. Macromol. Chem.* **1975**, *12*, 191.
(26) Kokai, F.; Kubota, T.; Ichjyo, M.; Wakai, K. *J. Appl. Polym. Sci., Appl. Polym. Symp.* **1988**, *42*, 197.
(27) Wells, R. K.; Badyal, J. P. S. *J. Polym. Sci., Polym. Chem. Ed.* **1992**, *30*, 2677.
(28) Laoharojanaphand, P.; Lin, T. J.; Stoffer, J. O. *J. Appl. Polym. Sci.* **1990**, *40*, 369.
(29) Hamada, K.; Morishita, H. *Spectrosc. Lett.* **1986**, *19*, 815.

Table II. Infrared Absorption Bands for Freshly Deposited TMS Plasma Polymer Powder[12,14,24,29-34] (W/F_M = 280 MJ/kg)

absorbance/cm^{-1}	assignment
2955	C–H asymmetrical stretching in CH_3
2926	C–H asymmetrical stretching in CH_2
2906	C–H symmetrical stretching in CH_3
2870	C–H symmetrical stretching in CH_2
1460	methyl asymmetric bending in CH_3–C
1375	methyl symmetrical bending in CH_3–C
1632	>C=C< stretching[a]
2110	Si–H stretching
1408	CH_2 symmetrical scissoring in Si-CH_2
1250	CH_3 symmetric bending in Si$[CH_3]_n$
1026	Si–O–Si and/or Si–O–C asymmetric stretching and/or CH_2 wagging in Si–$[CH_2]_n$–Si
833	CH_3 rocking in Si$[CH_3]_n$, n = 2, 3
791	CH_3 rocking in Si$[CH_3]_n$, n = 1, 2
685	Si–C stretching

[a] Supported by NMR results.

of this material to air for 1 month resulted in all of the above cited infrared absorption bands for the fresh powder shifting to slightly higher frequencies. This can be explained by the presence of trapped reactive centers in the solid participating in cross-linking and thereby increasing the amount of strain in the material.[30] Oxidation is also observed[35] with bands appearing at 3426 cm^{-1} (OH stretching[30]), 1707 cm^{-1} (C=O stretching[27]), and 1632 cm^{-1} (asymmetrical stretching mode of C=O in carboxylates or C=C stretching in unconjugated olefins[27]). The relative intensities of the 1250 cm^{-1} (CH_3 symmetric bending in Si$[CH_3]_n$) and 1026 cm^{-1} (Si–O–Si and/or Si–O–C asymmetric stretching and/or CH_2 wagging in Si–$(CH_2)_n$–Si) bands increase.

Figure 5 compares ATR infrared spectra of clean and coated polyethylene film as a function of W/F_M. Characteristic infrared absorbance bands for clean polyethylene film are assigned in Table III. Polyethylene coated with plasma polymer exhibits the following extra features: 2118 cm^{-1} (Si–H stretching), 1250 cm^{-1} (CH_3 symmetrical bending in Si$[CH_3]_n$), 1040 cm^{-1} (Si–O–Si and/or Si–O–C, and/or CH_2 wagging in Si–$[CH_2]_n$–Si), 834 cm^{-1} (CH_3 rocking in Si$[CH_3]_n$, n = 2, 3), 790 cm^{-1} (CH_3 rocking in Si$[CH_3]_n$, n = 1, 2), 689 cm^{-1} (Si–C stretching). One obvious difference between these spectra and their transmission counterparts is the attenuated plasma polymer C–H stretching bands. This can be explained in terms of there being a smaller depth of penetration at higher wavenumbers for the ATR technique, which in turn gives rise to weaker signal intensities.[38] Also the variable attenuation in the characteristic polyethylene bands can be explained in terms of infrared penetration depth being lower at higher wavenumbers (i.e., this region of the ATR–FTIR spectrum is more sensitive toward any surface modification). Low W/F_M values yield an increase in silicon related absorptions (Si–$[CH_2]_n$–Si, Si$[CH_3]_n$) with a concomitant loss of polyethylene C–H stretching bands.

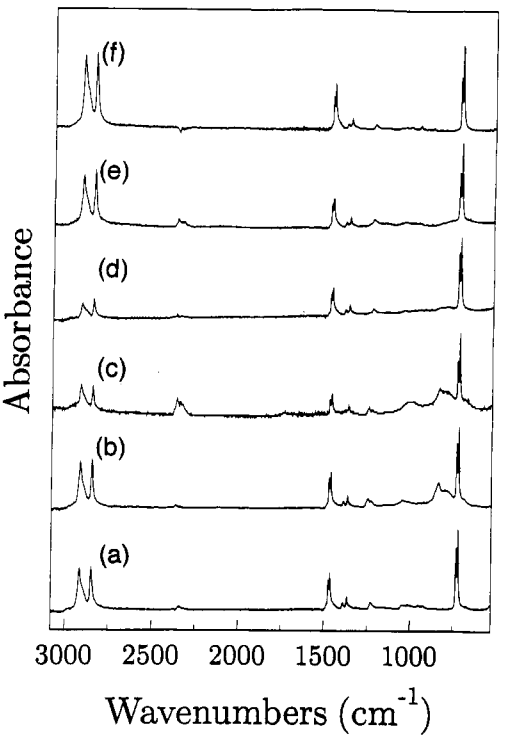

Figure 5. ATR-FTIR spectra of freshly deposited TMS plasma polymer onto polyethylene film for W/F_M values of (a) clean polyethylene, (b) 56 MJ/kg, (c) 140 MJ/kg, (d) 280 MJ/kg, (e) 560 MJ/kg, and (f) 1400 MJ/kg (10 min and 6.5 cm from monomer inlet).

Table III. Infrared Absorption Bands for Clean Polyethylene Film[30,35-37]

absorbance/cm^{-1}	assignment
2915	asymmetrical C–H stretching in CH_2
2847	symmetrical C–H stretching in CH_2
1472	CH_2 bending
1462	CH_2 bending
1366	CH_2 wagging and/or symmetrical CH_3 movements
729	CH_2 rocking
720	CH_2 rocking

As the glow discharge power increases, all silicon-related absorbances diminish, until eventually just polyethylene features remain. The greatest loss in intensity of the characteristic polyethylene peaks (2915 and 2847 cm^{-1}) occurs at approximately W/F_M = 280 MJ/kg; these experimental conditions correspond to the maximum deposition rate of plasma polymer and were therefore employed for powder formation.

Infrared spectra of coated polyethylene films located in different regions of the glow discharge are collated in Figure 6. The observed variation in organosilicon features imply that the rate of plasma polymerization drops on moving downstream from the precursor inlet.

Solid-State NMR. ^{13}C and ^{29}Si NMR spectra of fresh and aged TMS plasma polymer powder are shown in Figures 7 and 8, respectively. All NMR measurements are referenced to tetramethylsilane (TMS). Characteristic features observed in these spectra have been assigned in accordance with data published elsewhere.[30,31,39-42] ^{13}C and

(30) Painter, P. C.; Coleman, M. M.; Koenig, J. J. *The Theory of Vibrational Spectroscopy and Its Application to Polymeric Materials*; Wiley: New York, 1982.
(31) Tajima, I.; Yamamoto, M. *J. Polym. Sci., Polym. Chem. Ed.* **1987**, *25*, 1737.
(32) Cai, S.; Fang, J.; Yu, X. *J. Appl. Polym. Sci.* **1992**, *44*, 135.
(33) Coopes, I. H.; Griesser, H. J. *J. Appl. Polym. Sci.* **1989**, *37*, 3413.
(34) Wrobel, A. M.; Czeremuskin, G.; Szymanowski, H.; Kowalski, J. *Plasma Chem. Plasma Process.* **1990**, *10*, 277.
(35) Szeto, R.; Hess, D. W. *J. Appl. Phys.* **1981**, *52*, 903.
(36) Luongo, J. P.; Schonhorn, H. *J. Polym. Sci., Polym. Chem. Ed.* **1968**, *6*, 1649.
(37) Luongo, J. P. *J. Polym. Sci., Polym. Lett. Ed.* **1964**, *2*, 75.
(38) Mirabella, F. M. *Appl. Spectrosc. Rev.* **1985**, *21*, 45.
(39) Apperley, D. C.; Harris, R. K.; Marshall, G. L.; Thompson, D. P. *J. Am. Ceram. Soc.* **1991**, *74*, 777.
(40) Marsmann, H. *NMR: Basic Princ. Prog.* **1981**, *17*, 65.
(41) Fonseca, J. L. C.; Apperley, D. C.; Badyal, J. P. S. *Chem. Mater.* **1992**, *4*, 1271.
(42) Gamboji, R. J.; Cho, D. L.; Yasuda, H.; Blum, F. D. *J. Polym. Sci., Polym. Chem. Ed.* **1991**, *29*, 1801.

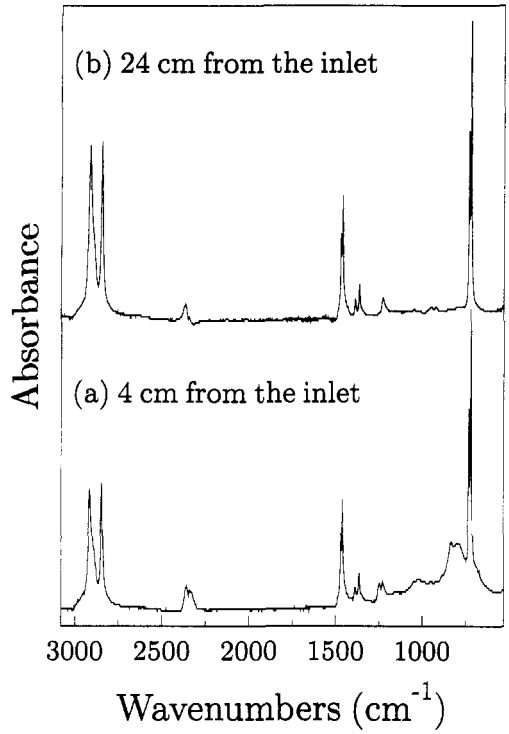

Figure 6. ATR-FTIR spectra of TMS plasma polymer coating deposited onto polyethylene film at (a) 4 cm and (b) 24 cm from the monomer inlet (W/F_M = 280 MJ/kg and 10 min).

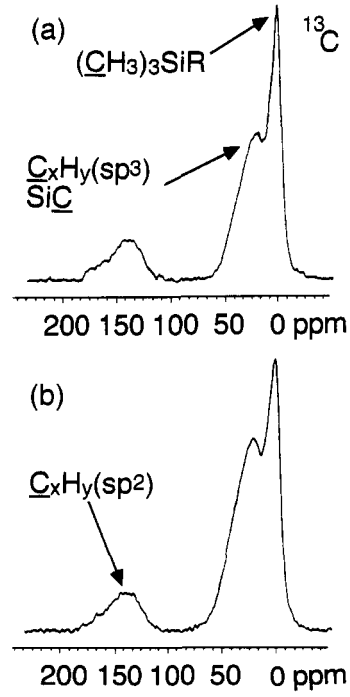

Figure 7. ^{13}C solid-state NMR spectra of (a) fresh and (b) aged TMS plasma powder (W/F_M = 280 MJ/kg).

^{29}Si peaks of greatest intensity are located at around 0 ppm. Therefore the major chemical environments present in the plasma deposit can be regarded as being similar to those known for the TMS reference compound.

A shoulder is evident in the ^{13}C NMR spectrum of fresh TMS plasma polymer powder (Figure 7) at approximately 20–50 ppm, this may be characteristic of either silicon carbide species[39] or sp^3 carbon atoms located within a hydrocarbon chain. Some degree of unsaturation in the plasma polymer is observed in the 120–180 ppm range (the occurrence of carbonyl groups in the fresh TMS plasma polymer is unlikely, since bulk oxidation was ruled out by XPS studies). It is of interest to note that this signal is much stronger than that found in the plasma deposit obtained from hexamethyldisilane precursor ($[CH_3]_3Si-Si[CH_3]_3$).[41]

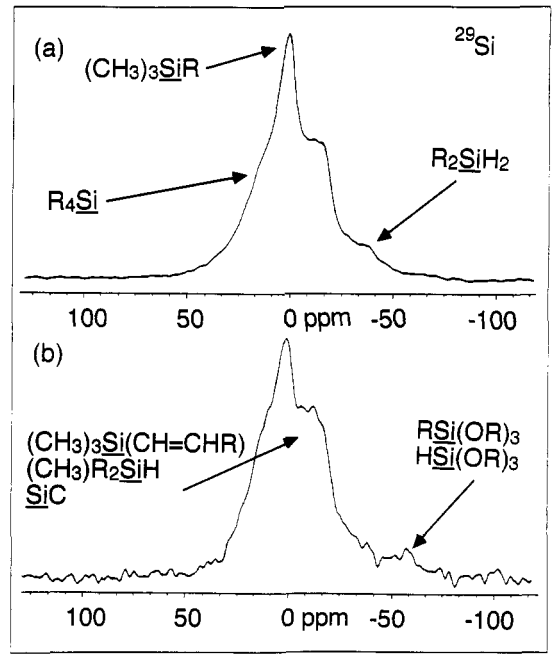

Figure 8. ^{29}Si solid-state NMR spectra of (a) fresh and (b) aged TMS plasma powder (W/F_M = 280 MJ/kg).

On leaving the collected material to age in air, there is an increase in intensity of the 20–50 ppm shoulder, which implies that a significant degree of cross-linking has taken place. A small number of alcohol functionalities in the 60–70 ppm region are also present.

The ^{29}Si NMR spectrum of fresh powder (Figure 8) consists of a strong signal centered at 1.8 ppm and a shoulder at −11 ppm range. The former is characteristic of $-Si[CH_3]_3$ fixed to hydrocarbon chain ends, and the latter can be attributed to one or more of the following: double-bond silicon environments (δ = −11.8 ppm for *cis*-$[CH_3]_3SiCH{=}CHSi[CH_3]_3$); or the presence of silicon carbide; or $(CH_3)R_2SiH$ provided R has an alkyl chain containing at least two $[-CH_2-]$ linkages (δ = −10.9 ppm for $[CH_3][n\text{-}C_3H_7]_2SiH$, δ = −9.8 ppm for $[CH_3][(n\text{-}C_4H_9)_2SiH]$, δ = −9.8 ppm for $[CH_3][n\text{-}C_5H_{11}]_2SiH$, δ = −9.9 ppm for $[CH_3][(n\text{-}C_6H_{13})_2SiH]$). The shoulder at +6.6 ppm is most likely to be silicon centers bonded to hydrocarbon chains where not more than one R chain is a methyl group (δ = +6.5 ppm for $[C_2H_5]_3Si[CH_3]$, δ = +7.1 ppm for $[C_2H_5]_3Si[C_2H_5]$, δ = +6.9 ppm for $[C_2H_5]_3Si[n\text{-}C_4H_9]$). The weak feature at −36.0 ppm could be some form of $R^1R^2SiH_2$ linkage (δ = −37.7 ppm for $[CH_3]_2SiH_2$).

The ^{29}Si NMR shoulders at 6.6 ppm, and −10 to −20 ppm increase during ageing; this can be ascribed to either cross-linking processes or the creation of more silicon carbide type linkages. In addition a weak peak is visible in the −50 to −80 ppm range, this can be assigned to the emergence of $RSi[OR]_3$ and $HSi[OR]_3$ environments.

Emission Spectroscopy. Figure 9 depicts the emission spectra of TMS plasmas at 5 W (140 MJ/kg) and 10 W (280 MJ/kg). Most of the lines in these spectra originate from electronic transitions within the hydrogen molecule (230–310-nm vibrational–rotational continuum, 363.3, 367.3, 379.9, 385.8, 387.1, 388.6, 406.1, 406.6, 406.9, 417.4, 420.1, 422.0, 433.8, 449.0, 449.6, 455.4, 458.0, 461.5, 463.2,

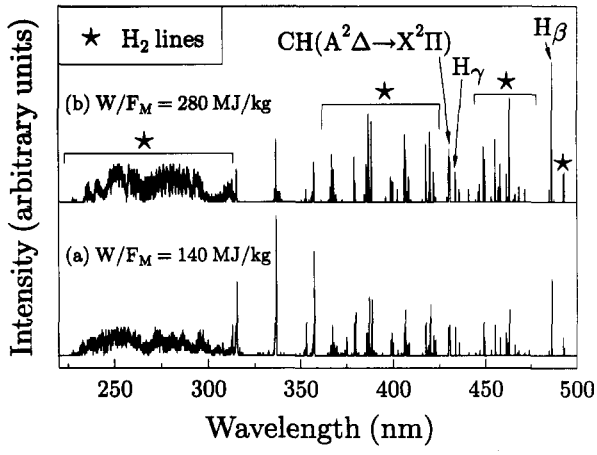

Figure 9. Emission spectra from TMS glow discharge at (a) W/F_M = 140 MJ/kg (5 W), and (b) W/F_M = 280 MJ/kg (10 W).

and 461.5 nm)[43,44] and hydrogen atom Balmer lines (486.1 and 434.1 nm).[45] These assignments were checked by running a pure hydrogen plasma. Other strong lines are due to the $C^3\Pi_u \rightarrow B^3\Pi_g$ transition for a nitrogen molecule:[46] 315.9 nm ($v' = 1$, $v'' = 0$), 337.1 nm (0, 0), and 357.7 nm (0, 1). It is important to take into consideration that these nitrogen lines are weaker by an approximate factor of 2000 compared to their intensity in a pure nitrogen plasma, and therefore the actual amount of molecular nitrogen in the reactor during TMS plasma polymerization must be less than 0.05 vol %. Finally, a band corresponding to the $A^2\Delta \rightarrow X^2\Pi$ transition for a CH radical was observed at 431.4 nm.[47,48] It proved impossible to assign any silicon-related features because of the intense hydrogen lines.

As the W/F_M value is increased from 140 MJ/kg (5 W) to 280 MJ/kg (10 W), all of the emission lines related to atomic and molecular hydrogen become relatively more intense. Therefore, a larger amount of atomic and molecular hydrogen is generated at higher powers due to greater fragmentation of the TMS molecule. Some gaps are evident within the molecular hydrogen 225–350-nm emission continuum at 238–240, 243–247, 255–258, 290–293, and 298–313 nm. The most likely explanation for these absences is that the TMS plasma medium contains unsaturated species which absorb strongly at these wavelengths. For instance, acetylene absorbs in the 220–240-nm range,[49,50] another possibility may be the propargyl radical (CH_2—C≡CH) which exhibits diffuse bands at 290–345 nm (strongest being at 332, 321.7, and 311.9 nm[51]), or perhaps diacetylene which has 700 narrow bands between 297 and 206.8 nm.[52]

Discussion

Plasma polymerization processes are widely regarded as being highly complex in nature. Typically they involve

Scheme I

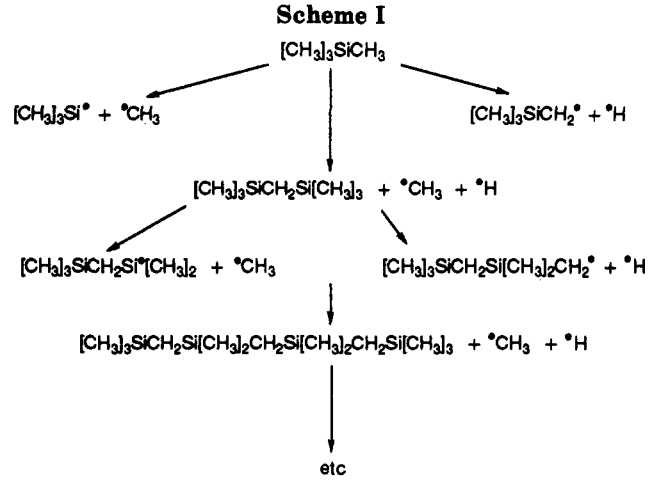

dissociation, generation, and recombination of polymerizable species within either the partially ionized gas itself and/or at the substrate surface.[1,53] Such reactions are perpetuated by electron impact and ultraviolet radiation. In simple terms

$$A\text{–}B \xrightarrow{e^-/h\nu} A^* + B^*$$

Where A and B may be individual atoms or molecular fragments which generate activated species A* and B* (ions and radicals). These intermediates can subsequently recombine to form new chemical species or impinge onto a growing polymeric layer. This description is appropriate for shorter deposition times; however, powdered material is generated over longer periods due to the high internal stresses associated with thicker coatings.[54,55] Such an explanation is supported by the observation that polyethylene films coated with thick TMS plasma polymer layers tend to curl up.

Bond energy values are as follows:[56,57] 292 kJ mol^{-1} (Si–C), 322 kJ mol^{-1} (Si–H), and 416 kJ mol^{-1} (C–H). Therefore Si–C and Si–H bonds are the weakest. Incorporation of $[CH_3]_nSi$ species into the plasma polymer (as detected by NMR, FTIR, and mass spectrometry[34]) is consistent with the cleavage of $[CH_3]_3Si\text{–}CH_3$ and $[CH_3]_3SiCH_2\text{-}H$ bonds; which leads to predominantly the primary reactions given in Scheme I.

Radical creation along the growing chain will result in branching, thereby creating a random three-dimensional network of $-[CH_3]_nSi-$ linkages. Weak Si–Si and strong C–C bonds may also form via homorecombination of carbon and silicon radicals, respectively. In TMS plasma polymer, a significant degree of unsaturation, cross-linking, Si–H groups, and possibly some embedded silicon carbide moieties were found. These products could originate from secondary interactions between electrons, ions, hydrogen atoms, and photons with the growing polymeric matrix. Additional unsaturated species may form via the plasma polymerization of methyl species generated during the primary fragmentation of the TMS molecule. Ageing is most likely to be a manifestation of trapped free-radical

(43) Pearse, R. W. B.; Gayon, A. G. *The Identification of Molecular Spectra*; Chapman and Hall: London, 1976.
(44) Dieke, G. H. *The Hydrogen Molecule Wavelength Tables of G. H. Dieke*; Crosswhite, H. M., Ed.; Wiley-Interscience: New York, 1972.
(45) Hollas, J. M. *Molecular Spectroscopy*; John Wiley & Sons: New York, 1987.
(46) *Spectroscopic Data Relative to Diatomic Molecules*; Rosen, B., Ed.; Pergamon: Oxford, 1970.
(47) Kiess, N. H.; Broida, H. P. *Astrophys. J.* **1956**, *123*, 166.
(48) Moore, C. E.; Broida, H. P. *J. Res. Natl. Bur. Stand.* **1959**, *A-63*, 19.
(49) Woo, S. C.; Liu, T. K.; Chu, T. C.; Chih, W. *J. Chem. Phys.* **1938**, *6*, 240.
(50) Innes, K. K. J. *Chem. Phys.* **1954**, *22*, 863.
(51) Ramsay, D. A.; Thistlewaite, P. *Can. J. Phys.* **1966**, *44*, 1381.
(52) Woo, S. C.; Chu, T. C. *J. Chem. Phys.* **1937**, 786.
(53) Bell, A. T. Fundamentals of Plasma *Chemistry*. In *Techniques and Applications of Plasma Chemistry*; Hollahan, J. R., Bell, A. T., Eds.; John Wiley & Sons: New York, 1974.
(54) Morinaka, A.; Asano, Y. *J. Appl. Polym. Sci.* **1982**, *27*, 2139.
(55) Clark, D. T.; Abrahman, M. Z. *J. Polym. Sci., Polym. Chem. Ed.* **1982**, *20*, 1729.
(56) Weast, R. C., Astle, M. J., Eds. *CRC Handbook of Chemistry and Physics*; CRC Press: Boca Raton, FL, 1982.
(57) Pilcher, G.; Leitão, M. L. P.; Yan, Y. M.; Walsh, R. *J. Chem. Soc., Faraday Trans.* **1991**, *87*, 841.

centers in the plasma polymer undergoing recombination or reacting with air, with perhaps some hydrolysis of Si–H bonds. There may possibly be silicon carbide species trapped within the organosilicon network, since the use of a heated substrate during plasma polymerization is reported to result in silicon carbide.[58]

In Park's empirical analysis of plasma polymerization kinetics,[59] overall deposition rate is described as being governed by an Arrhenius-type of activation energy E_a:

$$D_p \propto F_M \exp[-E_a/(W/F_M)]$$

where D_p is the average deposition rate along the whole reactor length. Using this model, for a fixed flow rate, the overall plasma polymer deposition rate should increase at higher W/F_M ratios toward a maximum value. In this study, the rate of TMS plasma polymerization at a local position in the reactor passes through a maximum with increasing W/F_M. This can be understood in terms of the mass flow rate (F_M) varying along the reactor length due to precipitation of plasma polymer (i.e., F_M drops on moving downstream), this will in turn influence the local deposition rate (Figure 10). For a given position in the reaction vessel, there will be no deposition in the absence of any electromagnetic field ($W = 0$) and also when there is a very low concentration of reactive species ($F_M = 0$). The latter situation will arise at high glow discharge powers, since virtually all of the polymerizable species will have been consumed upstream.

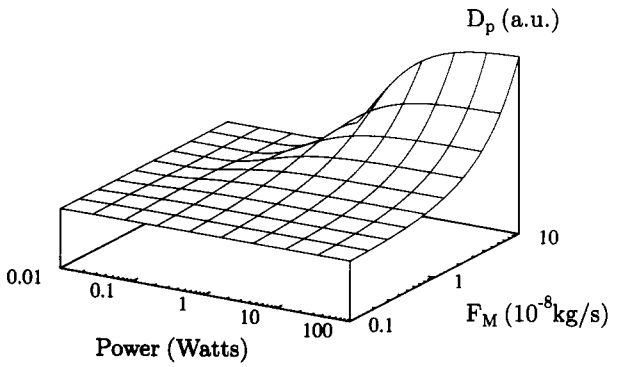

Figure 10. Dependence of deposition rate (D_p) on power and flow rate (F_m) calculated according to Park's empirical expression (E_a = 10 MJ/kg for illustrative purposes).

Conclusions

Plasma polymerization of tetramethylsilane at low powers and short periods result in continuous films, whereas longer times generate a coarse powder. The plasma polymer structure is believed to contain a random three dimensional network of $-[CH_3]_nSiH_m-$ linkages in conjunction with a significant degree of unsaturation, cross-linking, and possible some silicon carbide moieties. These materials undergo oxidation on storage in air.

Acknowledgment. J.L.C.F. thanks Brazil's Conselho Nacional de Desenvolvimento Científico e Tecnológico for financial support during the course of this work.

(58) Zhang, W.; Lelogeais, M.; Ducarroir, M. *Jpn. J. Appl. Phys.* **1992**, *31*, 4053.
(59) Park, S. Y.; Kim, N. *J. Appl. Polym. Sci., Appl. Polym. Symp.* **1990**, *46*, 91.